

DEVELOPMENT OF AN INNOVATIVE THREE-DIMENSIONAL COMPLETE BODY SCREENING DEVICE - 3D-CBS

D. B. CROSETTO

3D-Computing, Inc.

900 Hideaway Pl.

DeSoto, TX 75115, USA

E-mail: Crosetto@3d-computing.com

This article describes an innovative technological approach that increases the efficiency with which a large number of particles (photons) can be detected and analyzed. The three-dimensional complete body screening (3D-CBS) combines the functional imaging capability of the Positron Emission Tomography (PET) with those of the anatomical imaging capability of Computed Tomography (CT). The novel techniques provide better images in a shorter time with less radiation to the patient. A primary means of accomplishing this is the use of a larger solid angle, but this requires a new electronic technique capable of handling the increased data rate. This technique, combined with an improved and simplified detector assembly, enables executing complex real-time algorithms and allows more efficient use of economical crystals. These are the principal features of this invention. A good synergy of advanced techniques in particle detection, together with technological progress in industry (latest FPGA technology) and simple, but cost-effective ideas provide a revolutionary invention. This technology enables over 400 times PET efficiency improvement at once compared to two to three times improvements achieved every five years during the past decades. Details of the electronics are provided, including an IBM PC board with a parallel-processing architecture implemented in FPGA, enabling the execution of a programmable complex real-time algorithm for best detection of photons.

1. Introduction

Positron Emission Tomography (PET) is a medical imaging technique that detects and analyzes photons emitted after a patient ingests a radioactively tagged substance. The machine's electronics and computers transform the information into images that indicate metabolic activity. PET technology shows great potential for finding diseases such as the growth of cancer cells at the molecular level even before structural changes occur. Yet, high radiation doses have limited PET scans to patients with advanced disease. One full-body scan requires patient exposures to exceed 10 times the amount of radiation deemed acceptable for an entire year by the International Commission for Radiation Protection (ICRP). Today's PET scans can gather information on only one every 10,000 photons that are emitted because the electronic components become overwhelmed by data and do not have the capability to extract accurate

information (energy, arrival time and spatial resolution) of the photons hitting economical detectors. To compensate for those inefficiencies, current devices require radiation doses that surpass international guidelines.

Although PET technology has existed for 50 years, its benefits have never been fully realized. In addition to the radiation problem, increasing the narrow viewing field in a cost-effective manner so that full-body tests could be done quickly has been a stumbling block — until now.

The 3D-CBS will revolutionize health care, extending PET benefits to everyone, not just the gravely ill, because of its innovative data capture system, its larger detector, and a simpler manufacturing process. Those changes increase PET efficiency by a factor of more than 400 [1], [2], [3].

Advantages of the innovative technologies used in the 3D-CBS device:

- A lower radiation dose to a level acceptable by ICRP
- Shorter examination time, lower examination cost
- Superior image quality because of its accurate measuring capabilities of energy and spatial resolution (planar and depth), and photon's arrival time. Permits a more accurate diagnosis, reducing false positives and negatives
- Three-dimensional, whole-body, anatomical and functional imaging
- 3D-CBS has the unique capability of recording data continuously and simultaneously over the entire body. This makes it possible to view images of biological processes, blood flow, and organ movements as a video stream instead of a still picture.
- Improve the tracking of the clinical efficacy of therapy
- Test the effectiveness of experimental drugs, because of capability of recording data simultaneously over the entire body
- Screen for cancer at an earlier, more curable stage

2. The need for massively parallel processing for capturing more photons, more accurately in PET/CT

In order to understand where the photons were lost in a current PET device, and to understand what functions need improvement for increasing current PET efficiency, I made the study in the year 2000 and the results are summarised in [10], and in Figure 1.

2.1. Results of the study

The study shows that the lack in efficiency in PET was not due to inefficiency in crystals, as believed in the past, but rather it was due to the

inefficiency of the electronics, which also limits the detector assembly and the implementation of an efficient real-time photon-detection algorithm.

2.2. Solution to overcome the inefficiency of current PET

The solution to the limitations listed above is a massively parallel-processing system at the front-end electronics of the PET device such as the one described in Section 3. 3D-FlowTM parallel-processing architecture, which can be implemented in FPGA or ASIC. This parallel-processing system should not be confused with other types such as “Hypercube”, but rather it has the capability to execute a programmable digital-processing algorithm on each electronic channel with neighboring-signal correlation.

The 3D-FlowTM DAQ IBM PC board can trigger on any electronic channel based on the shape of the pulse received or based on the information of a cluster of pulses from several neighboring elements centered on the highest pulse (or local maxima). It can accurately measure incident photon energy by summing 9, 16, or 25 elements, eliminating scattered events and separating events from the different modalities (PET/CT). It can accurately measure the spatial resolution by interpolating the value of the sum of three (or more) elements to the left of the local maxima and three (or more) elements to the right for both the X and Y positions. The high parallelism of the internal units of the 3D-FlowTM processor allows executing complex real-time algorithms to accurately measure the depth of interaction (DOI) and eliminate parallax error of oblique photons. An oblique penetration of an incident photon into a crystal generates a parallax error if the DOI is not measured. During the past 14 years, different techniques have been used to measure the DOI. The digital signal processing capabilities of the 3D-FlowTM system offers the possibility of implementing several of these and more in addition.

Roderic Pettigrew, Director of NIBIB-NIH, during his talk at the plenary meeting of the IEEE-NSS-MIC conference on October 22, 2003, expressed the wish that the efficiency of PET would be increased 100 to 1000 times. Indeed, it is puzzling (as it is also reported by Brownell in the abstract of [1]) that, in the 50 years since the first Positron Imaging Device, and a long time after the invention of PET [2], so little progress has been made in adapting this technology to the needs of the health care industry. In science in general, important developments often remain unexploited for years or even decades after the initial work [1]. The inventions set forth in this document (and in previous documents [10], [9], [3], [4], [5]), now also verified by hardware implementation of the main components, remove the obstacles that have limited the improvement rate of PET efficiency to only 2 to 3 times every 5 years as in the past, allowing at once the improvement called for by Roderic Pettigrew.

2.3. Where the photons are lost in current PET

A detailed study of where the photons are lost in current PET is described in Figure 1. Before attempting to improve any system, it is necessary to determine where the inefficiencies are, how great they are, how they can be reduced, and by how much. Figure 1 is divided into six sections as follows:

Radiation dose: The initial number of pairs of photons emitted per second by the tracer in the patient's body (1424 million), represented in the upper left of Figure 1, and the number of pairs of photons per second captured by current PET (0.2 million), represented in the lower left of Figure 1 are not in question, because those quantities have been measured by hospitals and universities and are in accord with the measurements made by the PET manufacturers [6].

Section (1). Photons at start of the examination: Of the initial quantity of pairs of photons emitted from within the body, some 1210 million pairs per second are scattered or are absorbed in the body. Only 214 million pairs per second leave the body. This quantity of capturable photons, which is equivalent to 15% efficiency for the first stage, is supported by several simulations made by scientists at Los Alamos Laboratory and at universities in California and elsewhere (see references [7], [8]).

Section (2): Field-of-view (FOV): Photons from outside the detector area are lost, yielding an efficiency percentage figure equivalent to 8.5% for this stage. Applying this percentage to the 214 million pairs of photons per second leaving the body, only 18 million capturable pairs per second remain.

Section (3): Solid angle: Some photons from within the detector area are also lost. Only 3.2 million pairs of photons per second remain to be captured after stage 3, which is equivalent to 18% efficiency for this stage.

Section (4): Detector stopping power: Detector crystals do not have perfect stopping power and do not capture every photon in range. After stage 3 in some low-cost crystal detectors, 20% are lost, or 0.65 million, and 80% remain potentially capturable, or 2.5 million pairs per second.

Section (5-6) Electronics (combined to detector assembly): Calculation by subtraction. Current PET capture only 0.2 million pairs per second of the original 1424 million pairs of photons per second emitted by tracer within the patient's body (see measurements made by PET manufacturers and universities reported in scientific journals such as Figure 9 of reference [6]). Of the 2.6 million pairs of photons per second remaining after stage 4, the loss of 2.4 million pairs of photons per second is accounted for by deficiencies in the electronics and the detector design. The efficiency of stages 5 and 6 can be calculated as equivalent to 8%, as derived by subtraction from the total inefficiency and the sum of the other inefficiencies.

It is obvious from this analysis that the section that needs serious study and improvement is the last one, which provides only 8% efficiency. Section 1 has the efficiency related to a natural phenomenon that cannot be changed. Sections 2 and 3 can be increased in length and solid angle only if the electronics of sections 5 and 6 are not overwhelmed by the increased amount of data to be analyzed. Section 4, although it is the one in which much effort and money has been invested during the past decades, can only be improved from about 80% to something over 95%; crystals are already nearly ideal (such as LSO) and there is not much room for further improvement.

Changing the role of PET to screening for cancer								
Current PET systems				PET capabilities with the 3D-CBS				
Process affecting capture/loss of photons	Photons MBq		Efficiency at each stage	Radiation dose Reduced to 3%		Efficiency at each stage	Photons MBq	
	Remaining	Lost		Remaining	Lost		Remaining	
Radiation dose	1,424			Inject 66 mCi of ¹⁸ O-water = 1,424 MBq (at start of exam)	Inject 2.2 mCi of ¹⁸ O-water = 47.4 MBq (at start of exam)			47.4
Photons at start of scanning not scattered and/or absorbed in the body	214	1,210	15%	(1) 7% to 25% pair of photons in time coincidence leave the body		15%	40.3	7.1
Field-of-view (FOV) (photons from outside the detector area are lost)	18	196	8.5%	(2) FOV 16 cm Photons lost Photons captured	FOV 137.4 cm Photons lost Photons captured	95%	0.4	6.7
Solid angle (some photons from within the detector area are also lost)	3.2	14.8	18%	(3) Photons lost Photons captured	Photons lost Photons captured	92%	0.5	6.2
Stopping power (SP)	2.6	0.6	80%	(4) Crystal photon detection capability Photons → Crystal → Photon not stopped		80%	1.2	5
Electronics (photons captured)	0.2	2.4	8%	(5) Limitation of the electronics of current PET to identify "good" photons	Efficient photon identification with the 3D-Flow architecture	95%	0.3	4.7
				(6) Limitation of the electronics of current PET to identify photons in time coincidence	Efficient identification of photons in time coincidence by testing only detectors with hits			
0.014% Efficiency				0.2 million coincidences/sec found			4.7 million coincidences/sec found	10% Efficiency

Figure 1. shows the difference in efficiency between the current PET (left) and the 3D-CBS PET with the 3D-Flow™ (right). Areas of inefficiencies are detailed in Sections 1 through 6. Only the innovation of the electronics in sections 5 and 6 allow for the improvement in efficiency, in a cost-effective manner, in sections 2 and 3. (The column of MBq = million of pairs of photons per second, shows the numbers of photons lost and photons remaining at each Section, and the reduction applied as a percent of efficiency for that Section is found in the adjacent columns).

3. 3D-Flow™ parallel-processing architecture

This architecture takes the parallelization process one step further than DSP, and its software tools allow creation, in only a few hours, of a new application with different algorithms executed on thousands of processors. The high parallelism of the internal units of the 3D-Flow™ processor also allows executing complex real-time algorithms.

Each of the 3D-Flow™ processors of one layer of the 3D-Flow™ stack[°] (see Figure 2) executes in parallel the real-time algorithm, from beginning to end, on data received from the PET detector, while processors at different layers of the 3D-Flow™ stack operate from beginning to end on different sets of data received from the PET detector [9].

The 3D-Flow™ architecture extends the execution time in a pipeline stage beyond the time interval between two consecutive input data.

Rather than requiring an ultra fast, expensive technology capable to execute several special instructions (e.g., data moving and data processing such as the 26 operations of the 3D-Flow™) per second, or simplifying the real-time algorithm to the point that measurements such as energy, centroid, or DOI are not accurate, the 3D-Flow™ architecture permits the execution of complex algorithms and sustains a high input data rate using any technology (FPGA or ASIC at 0.25 micron or smaller, for enhanced performance at a higher cost).

The extension by the 3D-Flow™ architecture of the execution time in a pipeline stage beyond the time interval between two consecutive input data is illustrated by the following example: An identical circuit (a 3D-Flow™ processor) is copied four times (see Figure 2). (The number of times the circuit is copied corresponds to the ratio between the algorithm execution time and the time interval between two consecutive input data.) A bypass switch coupled to each processor in each 3D-Flow™ in layer A sends one data packet to its processor and passes three input data packets and one output result from its processor along to the next layer. The bypass switches on the 3D-Flow™

[°] The system architecture consists of several processors arranged in two orthogonal axes: One layer is an array of 3D-Flow processors, where each processor is interconnected to its four neighbors through North, East, West and South ports. Several layers, assembled one adjacent to another to make a system, is called a "stack." The first layer is connected to the input sensors, while the last layer produces the results processed by all layers in the stack. Data and results flow through the stack from the sensors to the last layer. An electronic channel consists of one set of 3D-Flow processors connected from the bottom port of one chip to the top port of an adjacent chip (with the top port of the first chip connected to the signal received from the detector and the bottom port of the last chip connected to the pyramid).

processors at layer B send two input data packets along to the next layer, one output result from received from layer A and one result from its processor, and so on. Only the processors at layer A are connected to the PET detector and these receive only input data. The processors at layer D send out only results. This architecture simplifies the connection in a parallel processing system and does not require a high fan-out from the detector electronics to send data to different processors of a parallel-processing system. All connections are point-to-point with several advantages in low power consumption, signal integrity, etc.

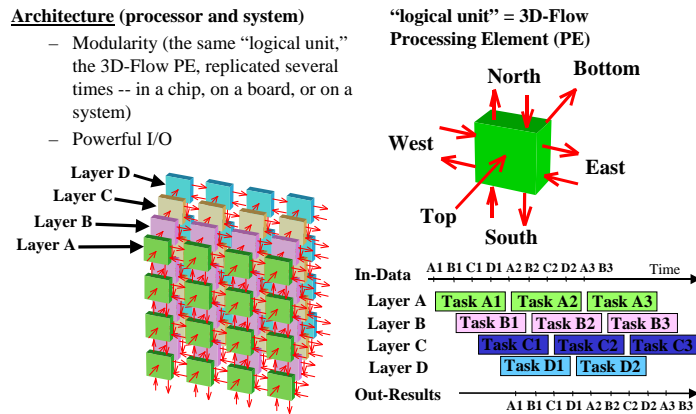


Figure 2. 3D-Flow™ parallel-processing architecture.

4. 3D-Flow™ DAQ IBM PC photon-detection board

The 3D-Flow™ DAQ IBM PC photon-detection board has the capability to execute different real-time algorithms for photon detection [10] and can be interfaced to different types of daughter analog-to-digital boards (ANIN_x). The daughter board provides signals carrying the amplitude information from an ADC (analogue to digital converter) and the time information from CFD-TDC (constant fraction discriminator and time to digital converter), for 16 detector channels (photomultipliers – PMT -- or avalanche photodiodes – APD --), coupled to different types of crystals (e.g., slow: NaI(Tl), BGO, or fast: LSO, GSO, etc.).

4.1. 3D-Flow™ DAQ Board specifications:

- 16 digital input channels (16-bit word-wide per channel);

- Two input clocks at 20 MHz and 40 MHz with internal PLL on each FPGA chip that provides the internal timing at 320 MHz.
- Two differential lines for output results (LVDS);
- Time to digital converter measuring photon's arrival time on each channel with resolution of 500 ps;
- Capability to execute in a programmable form, complex real-time algorithms with an execution time longer than the time interval between two consecutive input data. E.g. photon detection, DOI, graphic processing, etc.
- Capability of fast data exchange with neighboring 3D-FlowTM processors (North East, West, and South), which allows the correlation of signals that were split between several channels. This allows also clustering and local maxima calculation.
- Capability to trigger on any channel that has been acquired and processed in parallel on all channels with zero dead-time.
- Capability to funnel results from 16 input channels to one (or two) output channels via routing algorithms executed on 20 processors 3D-Flow-pyramid accommodated in 5 FPGA chips.
- Four serial I/O interfaces for 3D-FlowTM program loading, initialization, and system monitoring during data taking
- PCI interface;
- The testability with a) a JTAG chain through the 29 large components; b) 70 LED; c) 120 test points at a 120-pin connector, and d) 50 test points scattered at different locations on the board, which permit monitoring/debugging of critical functions/timing;
- The board is designed to work: a) 'stand-alone', to process data at a high rate, b) in a system made of several boards only controlled by RS232, or c) stand-alone or in a system controlled by PCI interface.
- The board is designed and implemented in such a way that any clock pin of any 3D-FlowTM FPGA chip in any board of the system (even when the boards belong to different crates or chassis) will not have a skew with any other 3D-FlowTM FPGA clock pin that will exceed 40 ps.

4.2. 3D-FlowTM DAQ Board Implementation:

I designed the 3D-FlowTM DAQ IBM PC photon detection board (see Figure 3 and Figure 4) with Concept HDL (Cadence). A commercial autorouter could not route the layout automatically, with connections of 2,211 components with over 20,000 pins, in less than 16 layers, which is the limit for standard IBM PC board thickness. After some study, I solved the problem by placing the components in a particular location on the board and by a special assignment of the signals to the pins that would facilitate the routing, avoiding many vias and crossing connections. The board could then be successfully routed in part

manually with Allegro (Cadence) and in part with the autorouter Spectra (Cadence) in only eight layers of signals. Particular attention was paid to the power distribution, using six ground and power planes. I had also paid particular consideration to the clock distribution, which was implemented so that two clocks correlated in phase are distributed from a single source to all components in different boards with a maximum skew of only 40 picoseconds between any two clock signals in the 3D-Flow™ processors in any place of the system. The printed circuit (PCB) of the photon-detection board was manufactured by one of the foremost companies manufacturing PCB for high-end technological applications. Some components were received as free samples, and I had the board assembled by a company that uses the most reliable processes (e.g. automatic pick and place of the components and temperature controlled soldering flow). Both companies are thoroughly familiar with regulations needed to comply with electronics for medical equipment and have among their customers companies that manufacture medical equipment.

The board is of reliable construction and I have used intentionally only through-hole vias (no blind or buried vias were used) in order to keep the fabrication cost low (for an order of 100 pieces, the cost per PCB board is estimated at \$70).



Figure 3. Top view of the 3D-Flow™ DAQ IBM PC photon detection board.

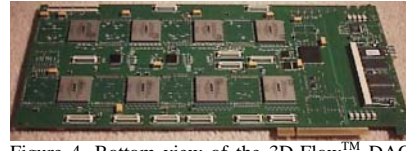


Figure 4. Bottom view of the 3D-Flow™ DAQ IBM PC photon detection board.

Figure 5 shows the main hardware components of the 3D-CBS which are:

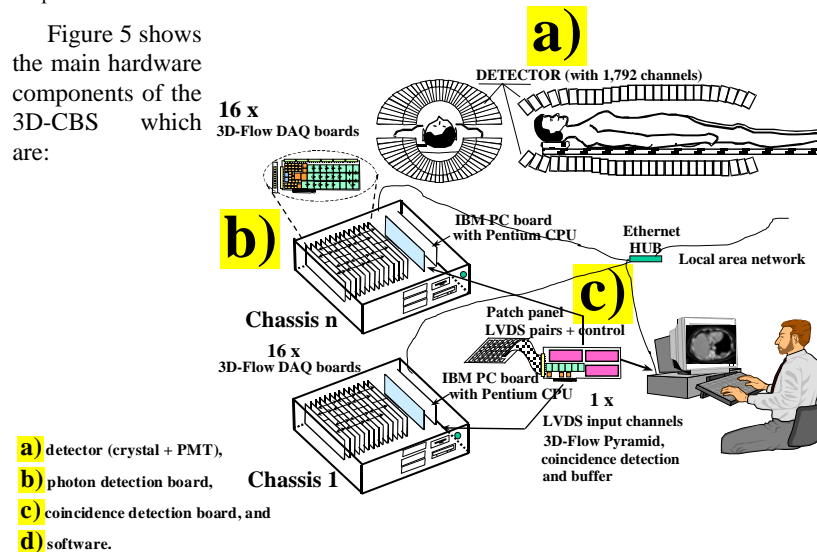


Figure 5. Layout of the hardware assembly of the 3D-CBS.

The detector can be purchased off the shelf. A prototype of the photon detection board for 16 channels (see Figures 3, 4) was built. The coincidence detection board (center in the figure), is designed and under construction. The real-time software for trouble-shooting during operation has been developed.

The two-dimensional board (printed circuit board –PCB–) of Figure 3, 4 implements the three-dimensional parallel-processing architecture of 64 processors as shown in Figure 1. (The board has four extra processors compared to the drawing in Figure 1, which implement the funneling in the pyramid of the system). The array can be expanded in size virtually indefinitely by plugging more boards into a chassis (up to 16 per chassis) and stacking more chassis in racks. The details of the concept of such a massively parallel-processing system and the blue print of the practical implementation are provided in the book [10].

4.3. Acknowledgments

I wish to thank Dr. Michele Barone and Dr. Pier Giorgio Rancoita for the invitation to the ICATTP conference and the Session organizer Dr. T.J. Ruth.

References:

-
- [1] Brownell, LG.: "A History of Positron Imaging." Physics Research Laboratory, Massachusetts General Hospital, MIT. October 15, 1999. See also website <http://www.mit.edu/~glb/alb.html>.
 - [2] Webb, S.: "From the Watching of Shadows: The Origins of Radiological Tomography" ISBN 085274305X
 - [3] Crosetto, D. Saving lives through early cancer detection: Breaking the curr. PET eff. Barr. with the 3D-CBS." www.3d-computing.com/pb/3d-cbs.pdf.
 - [4] Crosetto, D.: "The 3-D Complete Body Screening (3D-CBS) Features and Implementation" IEEE-NSS-MIC-2003. Conference Record. M7-129.
 - [5] Crosetto, D.: "Channel Reduction and Time Coincidence IBM PC board for PET" IEEE-NSS-MIC-2003. Conference Record. M6-131.
 - [6] DeGrado, T.R., et al.: Performance Characteristics of a Whole-Body PET Scanner, *Journal of Nuclear Medicine*, vol. 35(8):1398-1406, Aug. 1994,
 - [7] Tumer, O. Tumay, U.S. Patent No. 5,821,541. Method and apparatus for radiation detection.
 - [8] Hughes, H.G., et al.: MCPNPX-The LAHET/MCNP Code Merger. XTM-RN(U) 97-012, Los Alamos National Laboratory; 1997.
 - [9] Crosetto, D.: LHCb base-line level-0 trigger 3D-Flow impl. *Nuclear Instr. & Methods in Physics Research, Sec. A*, vol. 436 (1999) pp. 341-385.
 - [10] Crosetto, D.: 400+ times improved PET efficiency for lower-dose radiation, low-cost cancer screening. ISBN 0-9702897-0-7. Available at Amazon.com